Received: 16 May 2023 | Accepted: 31 December 2023

DOI: 10.1111/ede.12469

RESEARCH ARTICLE

WILEY

The evolution of cnidarian stinging cells supports a Precambrian radiation of animal predators

Noémie C. Sierra[1,2] | **David A. Gold**[1,2]

[1]Department of Earth and Planetary Sciences, University of California, Davis, Davis, California, USA

[2]Integrative Genetics and Genomics, University of California, Davis, Davis, California, USA

Correspondence
David A. Gold, Department of Earth and Planetary Sciences. University of California, Davis. Davis, CA, USA.
Email: dgold@ucdavis.edu

Funding information
National Science Foundation

Abstract

Cnidarians—the phylum including sea anemones, corals, jellyfish, and hydroids—are one of the oldest groups of predatory animals. Nearly all cnidarians are carnivores that use stinging cells called cnidocytes to ensnare and/or envenom their prey. However, there is considerable diversity in cnidocyte form and function. Tracing the evolutionary history of cnidocytes may therefore provide a proxy for early animal feeding strategies. In this study, we generated a time-calibrated molecular clock of cnidarians and performed ancestral state reconstruction on 12 cnidocyte types to test the hypothesis that the original cnidocyte was involved in prey capture. We conclude that the first cnidarians had only the simplest and least specialized cnidocyte type (the isorhiza) which was just as likely to be used for adhesion and/or defense as the capture of prey. A rapid diversification of specialized cnidocytes occurred through the Ediacaran (~654–574 million years ago), with major subgroups developing unique sets of cnidocytes to match their distinct feeding styles. These results are robust to changes in the molecular clock model, and are consistent with growing evidence for an Ediacaran diversification of animals. Our work also provides insight into the evolution of this complex cell type, suggesting that convergence of forms is rare, with the mastigophore being an interesting counterexample.

KEYWORDS
animal origins, cnidarians, cnidocyte, evolution of carnivory, Precambrian

1 | BACKGROUND

Cnidarians are one of the oldest living groups of carnivorous animals. With over 10,000 described species, cnidarians demonstrate a dizzying array of morphologies, ecological roles, and life history strategies, yet they are unified by the presence of a cell type called the cnidocyte (Figure 1). Cnidocytes are colloquially called "stinging cells," as they allow cnidarians to deliver their infamous painful, venomous stings. The cnidocyte is one of the most complex animal cells, and it has become an emerging model system for the evolution of novel cell types (Babonis & Martindale, 2014). They are dominated by a single, pressurized organelle called a capsule, which houses a coiled, hollow tubule. When triggered, the tubule can be discharged from the cell at microsecond-timescales with a force greater than 500,000,000 g (Nüchter et al., 2006). This force allows the tubule to penetrate the tissue of other animals, and many cnidocyte tubules are barbed and/or associated with toxins. These toxins have a biochemical complexity of their own, which can vary dramatically even in morphologically similar cnidocytes (Columbus-Shenkar et al., 2018). Nearly all living cnidarians use cnidocytes for prey capture, generally feeding on zooplankton or larger animals. The complexity of cnidocytes and their ubiquity across the Cnidaria strongly suggests that their last common ancestor

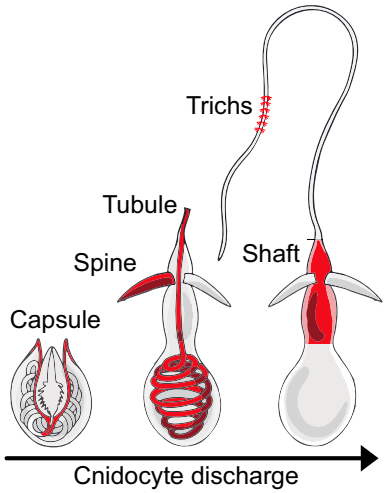

FIGURE 1 The general structure of a cnidocyte, based on the stenotele form. The images from left to right demonstrate the process of cnidocyte discharge (or firing). Components of the cell discussed in this paper are labeled and colored red.

also harbored cnidocytes. Yet, molecular clocks and fossil data suggest that the first cnidarians evolved in the Neoproterozoic (~100–539 million years ago [mya]), well before the diversification of the bilaterian animals they currently feed on (Erwin et al., 2011; Iten et al., 2016; Liu et al., 2014). This begs the question; what were the earliest cnidarians doing with stinging cells if there was no prey to sting?

Although cnidocytes are best known for ensnaring and/or envenomating prey (Boillon et al., 2004; Damian-Serrano et al., 2021; Kass-Simon & Scappaticci, 2002), they come in a variety of forms with distinct functions. This includes substrate attachment (Siddall et al., 1995), construction of tube-dwellings (Mariscal, Conklin, et al., 1977), self-defense/intraspecific competition (Kass-Simon & Scappaticci, 2002), and mating (Garm et al., 2015). The parasitic myzoxoans even use their cnidocytes to anchor themselves to their hosts and initiate infection (Americus et al., 2020; Ben-David et al., 2016). Reflecting these different functions, cnidocytes are extremely diverse, with over 30 "types" currently described. Historically, cnidocytes have been organized based on their morphology and used as a tool for cladistics (Bouillon et al., 2004; Gershwin, 2006; Östman, 2000). Classification systems of cnidocytes have varied across studies as new types are identified and microscopy techniques improve, allowing for nuanced discussions of the location, size, and shape of barbs (or trichs), the position of swellings along the shaft, and the pleating within the capsule (Mariscal, Conklin, et al., 1977). However, the inconsistency of classification schemes and descriptions makes understanding the relationships of cnidocyte types a challenge. Most cnidarian species have more than one type of cnidocyte, and their repertoire—known as the cnidome—can change over their lifetime, often in association with diet and ecological niche (Carrette et al., 2002; Purcell, 1984; Zenkert et al., 2011). Still, this diversity of cnidocyte form and function provides a potentially useful tool; by reconstructing the evolutionary history of this cell type we should be able to constrain its original function and determine when new ecological capabilities evolved in Cnidaria.

2 | METHODS

2.1 | Tree selection

Analyses were performed on a fossil-calibrated molecular clock based on a gene tree sourced from Picciani et al. (2018) (file: https://github.com/npicciani/picciani_et_al_2018/blob/master/Analyses/10_Time_calibration/tree_cnid_635.tre). This tree was selected because of high species coverage (1106 cnidarians) and the availability of associated genetic data (a minimum of two genes for each species on the tree). Some aspects of the topology were manually corrected using Mesquite v.3.51 to reflect current knowledge about higher taxonomic relationships. Specifically, the tree was manually edited to change the relationships within medusozoa to (Hydrozoa, [Staurozoa, {Cubozoa, Scyphozoa}]) based on Kayal et al. (2018), Zapata et al. (2015) and outgroup relationships were adjusted to (Porifera, (Placozoa, [Cnidaria, {Deuterostomia, Protostomia}]) based on Laumer et al. (2019). Because cnidomes can vary even between sister species, undescriptive species (such as species names "spp") were pruned from the tree. This species list was used to query the WoRMS database (accessed on October 29, 2021) to update species nomenclature, resulting in 904 cnidarian species plus four outgroups. We considered adding the unrepresented, parasitic Myxozoa to our data set, but ultimately decided against it for several reasons. First, the group has morphologically distinct cnidocytes called polar capsules, meaning their inclusion would not be informative for inferring the ancestral cnidarian cell type. Second, including this highly degenerate and poorly sampled clade in our molecular clock would likely lead to the overestimation of divergence times. This study therefore limits itself to the major clades of free-living cnidarians.

2.2 | Cnidome data collection

The cnidome of each species was determined from literature searches, with a focus on the 904 species in the starting tree. The results of this search are available in Supporting Information S1: Table S1. When conflicting

cnidome data occurred in the literature, we prioritized (1) multiple separate observations over stand-alone observations, (2) cnidome surveys over individual species reports, and (3) microscopy-based assignments over drawings and/or written descriptions. We ultimately recovered cnidocyte data for 477 species, and the data was converted to binary (absence = 0, presence = 1) format for each cnidocyte type. While as many as 30 cnidocyte types have been described (Mariscal, 1974a; Tardent, 1995) we restricted our analyses to 13 types that occurred in more than three species in our data set, and whose definition has been consistent over the last century. We also excluded tumiteles, mesoteles, and trirhopaloids from our analysis, as they did not appear in a sufficient number of species on our tree for meaningful ancestral state reconstruction.

2.3 | Molecular clock analysis

The molecular clock was produced using BEAST v1.10.4 (Suchard et al., 2018). Genetic data was downloaded from the GitHub account associated with Picciani et al. (2018) (file: "3_processed_alignments.fa"). Species names were adjusted to match changes to the tree, and NCBI accession numbers were removed from headers. All 908 species in the pruned tree were used for this analysis. Although only 477 species contained cnidocyte data (and therefore could be used in the ancestral state reconstruction) we included all taxa for the molecular clock to provide more data and ideally improve resolution. IQTree v1.6.12 (Kalyaanamoorthy et al., 2017; Minh et al., 2020) was run on each separate gene alignment to determine the optimal substitution model for each gene. Genes were then concatenated into a single supermatrix for use with BEAST.

Calibrations for seven nodes were set based on data from the fossil record (Supporting Information S1: Table S2) (Baron-Szabo et al., 2006; Dong et al., 2013; Ezaki, 2000; Fedonkin & Waggoner, 1997; Fuller & Jenkins, 2007; Han et al., 2010, 2016; Jell et al., 2011; Johnson & Richardson, 1968). Age ranges for the calibrated nodes were modeled under a lognormal distribution, using a lower (younger) bound from the fossil record and an upper (older) soft bound based on a lognormal probability curve. A starting chronogram consistent with these calibrations was generated using the starttree script (included in the GitHub project folder). A Yule model of speciation was chosen given the incompleteness of species represented in the tree. For the Bayesian analysis, two chains were run for 10,000,000 generations, logging the results every 1000 generations. A consensus chronogram from the two runs was produced with the TreeAnnotator application packaged with BEAST, using a 25% burnin and mean node heights. The XML file used to run BEAST is provided on GitHub.

A second, more conservative molecular clock was generated from the same data set. In this setup, hard lower bounds were set for the age of bilateria (636.1 mya), Cnidaria (636.1 mya), and animals (833 mya) based on recommendations from the Fossil Calibration Database (Benton et al., 2015). Any lognormal prior distributions from our original fossil calibrations that exceeded these lower bounds were converted into uniform priors constrained between the age of the fossil and the hard lower bound. A local clock model was used instead of a relaxed lognormal clock, which required an unlinking of the clock and site models for each gene in the data set. The results from this second analysis produced date estimates for Hydrozoa that were inconsistent with the fossil record. We therefore re-ran the clock, adding an additional calibration for the Leptothecata using the upper-Cambrian hydroid *Palaeodiphasia* (Song et al., 2021). After the additional calibration was added, we ran the clock in triplicate, with each run including two chains and 10,000,000 generations, logging the results every 1000 generations. The results were combined using the LogCombiner application packaged with BEAST, with a 25% burnin for each data set. A consensus tree was generated using the TreeAnnotator application packaged with BEAST, using mean node heights.

2.4 | Ancestral state reconstruction

The chronogram from BEAST was pruned to the 477 species with cnidocyte data using phytools v0.7.80 (Revell, 2014). Model testing was performed using the pruned chronogram and binary character data for each cnidocyte using the R package corHMM v2.7 (Beaulieu et al., 2020). For each cnidocyte type we compared four substitution models: (1) an equal-rates model (ER) with 1 hidden rate category (2) an ER model with two hidden rate categories (3) an all-rates-different model (ARD) with one hidden rate category, and (4) an ARD model with two hidden rate categories (for details on hidden rates models, see Boyko and Beaulieu [2021]). The resulting rate matrices are provided in Supporting Information S1: Table S3. Model preference was assessed using AIC criteria. The rate matrix for each model (ER1cat, ER2cat, ARD1cat, and ARD2cat) was created following the corHMMv2.1 vignette on CRAN (https://cran.r-project.org/web/packages/corHMM/) and provided in Supporting Information S1: Table S4.

Stochastic mapping was used to simulate evolutionary histories along the time-calibrated phylogeny, using the preferred model of evolution for each analysis as predicted by corHMM. The specific data for each model (rates, stationary frequencies, etc) for each cnidocyte was retrieved from the corHMM output and set as the model input for stochastic mapping using corHMMv2.7::makeSimmap(). The character data was formatted for input with the script 0_data_cleanup.Rmd. The root prior of the tree was initialized as 0 (absent) for each cnidocyte, under the assumption that cnidocytes were not present in the last common ancestor of animals. The analysis was run with 10,000 histories. The stochastic mapping results were then converted to phytools format using functions available from thackl/thacklr (https://rdrr.io/github/thackl/thacklr/src/R/phylo.R) and summarized using phytools::describe.simmap(). Plot summaries were generated for the internal node results (sim.obj$ace results) demonstrating the frequency at which each node was in each state (presence or absence, within hmm1 or hmm2 in relevant two category hmm cases) and producing a density map demonstrating the frequency of transitions within the branch length.

3 | RESULTS

The results of our analyses are summarized in Figure 2 and Supporting Information S1: Tables S4 and S5. In this section, we break down the results for each cnidocyte type, summarizing its morphology and evolution. We organize cnidocyte types by their origin, starting with those found across the cnidarian tree, and then focusing on those that are more taxonomically restricted. We conclude this section by considering how a more conservative molecular clock impacts our results. Ultimately, we provide robust support for the hypothesis that a radiation of cnidocyte types occurred in the late Neoproterozoic, right before the explosion of animal fossils in the Cambrian and the start of the modern, Phanerozoic Eon.

For clarity, the first time we refer to a taxonomic clade in the remaining text, we include the names of two species in our tree whose last common ancestor defines the group. We also include the date of that last common ancestor based on our molecular clock, resulting in the following format: "taxonomic clade" ("species 1" + "species 2"; "95% confidence interval on ancestral node in 'mya', or millions of years ago"). We chose $p = .7$ as a

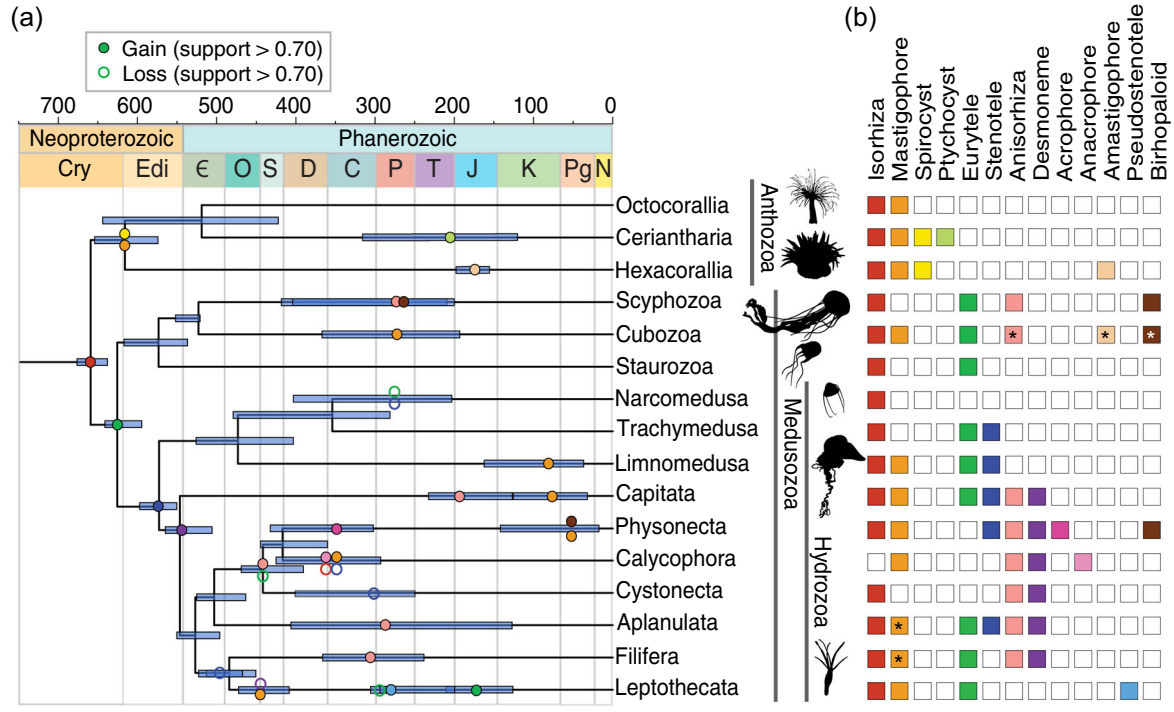

FIGURE 2 Graphic summary of cnidocyte analysis. (a) A molecular clock of cnidarians, with colored circles at nodes noting the timing of important gains and losses of cnidocyte types. The color of each circle signifies cnidocyte types, as detailed in section (b). Purple bars represent 95% confidence intervals for the divergence time of the represented node. Cry, Cryogenian; Edi, Ediacaran; Є, Cambrian; O, Ordovician; S, Silurian; D, Devonian; C, Carboniferous; P, Permian; Tr Triassic; J, Jurassic; K, Cretaceous; Pe, Paleogene; N, Neogene. (b) The distribution of cnidocyte types in the major lineages of cnidarians visualized as a presence/absence matrix. Boxes that contain asterisks indicate that the cnidocyte type was too rare in our data set to determine the timing of its origin.

semiarbitrary probability cutoff. This balances our desire for confidence with the observation that uncertainty naturally increases at deeper nodes of the tree. Detailed output for each ancestral state reconstruction can be found in Supporting Information S1: Figures S1–S13.

3.1 | Cnidarian-wide cnidocytes

We recovered three types of cnidocytes that were present across the major cnidarian clades, but only one type—the isorhiza—could be identified in the last common ancestor with statistical confidence ($p \geq .7$).

3.1.1 | Isorhiza

Isorhiza are the morphologically simplest and most ubiquitous cnidocytes, characterized by an isodiametric thread and no shaft. In our analysis, isorhiza were the only cnidocyte with statistical support for being present ($p = .70$) in the last common ancestor of Cnidaria (*Abietinaria filicula* + *Abyssoprimnoa gemina*; 676–637 mya). We consider the implications of this finding in the discussion.

3.1.2 | Mastigophores

Mastigophores are characterized by a shaft, or a cylindrical enlargement of the thread proximal to the capsule (see Figure 1; Carlgren, 1940; Mariscal, 1974a; Östman, 2000; Tardent, 1995). Mastigophores are ubiquitous within the sampled Anthozoa (*A. gemina* + *Epizoanthus illoricatus*; 654–574 mya), and common in Hydrozoa (*Aegina citrea* + *A. filicula*; 597–552 mya). Mastigophores have also been described in some Cubozoa (*Alatina moseri* + *Chiropsalmus quadrumanus*; 467–409 mya). Our analysis did not provide strong support for mastigophores in the last common ancestor of Cnidaria ($p = .47$), suggesting they evolved independently multiple times. The first well-supported appearance of mastigophores is in the last common ancestor of Anthozoa ($p = .82$) sometime between the end-Cryogenian and early Ediacaran. Our analysis suggests the mastigophores, with its increase in cnidocyte thread complexity, evolved at least eight times in the Cnidaria.

3.1.3 | Amastigophores

The amastigophore possesses a cylindrical and pointed shaft similar to that of the mastigophore, but it lacks a tubule. While a small tubule may be visible in the undischarged cnidocyte (Cutress, 1955; Östman, 2000) upon discharge the distal tubule breaks off at or close to the shaft (Östman, 2000) so that no distal tubule (Carlgren, 1940; Mariscal, 1974a; Östman, 2000) or a very short one (Fautin, 2009) is visible after discharge. These cnidocytes are present in several species of Cubozoa and Anthozoa. Our analyses strongly suggest that amastigophores evolved convergently multiple times in both classes, as the probability of their presence at their last common ancestor is $p = .00$. Amastigophores were too rare in cubozoans to estimate an origin; in Anthozoans they first evolved sometime in the Jurassic (Figure 2). Our analysis suggests the amastigophore, with its moderate loss of cnidocyte tubule complexity, evolved at least four times in the Phanerozoic.

3.2 | Anthozoan-specific cnidocytes

Anthozoans (corals and anemones) lack the swimming medusa stage found in their sister clade, the Medusozoa (Figure 2). In our analysis, two cnidocyte types were exclusive to anthozoans, the spirocyst and ptychocyst.

3.2.1 | Spirocysts

Spirocysts are adhesive cnidocytes lacking spines which upon eversion create a web of fine, adhesive fibrils (Mariscal, McLean, et al., 1977; Rifkin, 1991). They are nearly ubiquitous among the Hexacorallia (*Acanthopathes thyoides* + *E. illoricatus*; 589–513 mya) and Ceriantharia (*Ceriantheomorphe brasiliensis* + *Isarachnanthus nocturnus*; 314–117 mya). Our results provide strong support for spirocysts being present in the last common ancestor of Anthozoa ($p = .90$), and little support for their presence in the last common ancestor of Cnidaria ($p = .01$). We note that the placement of Ceriantharia is contentious; if our topology is incorrect, then spirocysts would be a hexacoral novelty that evolved slightly later. Regardless, our results suggest that the spirocyst, with its modified tubule armature, evolved once in the Neoproterozoic.

3.2.2 | Ptychocysts

Ptychocysts are used in construction by tube-dwelling anemones of the subclass Ceriantharia, and are characterized by a pleated, rather than helical, organization of the tubule thread. First described by Carlgren, (1912, 1940) and Schmidt (1974) as "atrichs" (atrichous

isorhiza), they were eventually distinguished by Mariscal, Conklin, et al. (1977) as a separate type due to the visible folds in the length of the tubule which likely help to intertwine the discharged threads forming a tightly woven mesh around the anemone. Our results support the hypothesis that ptychocysts are a novelty of the Ceriantharia (*Cerianthus membranaceus* + *C. brasiliensis*; 256–117 mya). Our results suggest that the ptychocysts, with its modified tubule morphology, evolved once in the Phanerozoic.

3.3 | Medusozoan-specific cnidocytes

Unlike anthozoans, many medusozoans (jellyfish, hydroids, siphonophores, and their relatives) contain a swimming, sexually reproductive medusa life stage. The prevailing hypothesis is that the earliest cnidarians lacked a medusa stage (Kayal et al., 2018) although research on genomes and gene expression patterns in some medusozoans may challenge this hypothesis (Gold, Katsuki, et al., 2019; Leclère et al., 2019). Regardless, the medusa life stage is associated with a diversification of feeding strategies, and thus a greater range of cnidocyte types.

3.3.1 | Euryteles

Gershwin (2006) notes that the name "eurytele" has been interchangeably used to represent either cnidocytes with a single swelling along the shaft, or a distal swelling on the shaft (this despite the Greek etymology: *eury* = widened *tele* = distal). Unfortunately, the absence of images in some relevant scientific papers prevented us from testing the evolution of different subtypes. Under the assumption that all euryteles are homologous, our results strongly support the hypothesis that euryteles are a medusozoan novelty, with a high degree of support for its presence in the last common ancestor of Medusozoa ($p = .99$) and very low support for its presence in the last common ancestor of Cnidaria ($p = .02$) We identified several potential instances of re-evolution, such as within Kirchenpauridae (*Oswaldella stepanjantsae* + *Kirchenpaueria pinnata*, 212–128 mya), where euryteles were most likely absent in an ancestral clade (*Aglaophenia elongata* + *A. filicula*, 307–288 mya; $p = .08$) but reappear with strong support ($p = .99$). The eurytele may therefore provide an example of a complex morphology evolving more than once, but uncertainty about the cell type's definition makes it difficult to make such a claim without further research. Regardless, the earliest euryteles evolved in the Neoproterozoic with the origin of medusozoans.

3.3.2 | Birhopaloids

Birhopaloids are characterized by the presence of two swellings within the shaft (Gershwin, 2006; Östman, 2000). These cell types are present in several species of Scyphozoa, hydrozoan siphonophores, and one cubozoan in our data set. Our analysis rejects the hypothesis that birhopaloids were present in the ancestor of Medusozoa ($p = .00$), suggesting this cell type evolved independently in each clade. The earliest well-supported appearance of birhopaloids is within the Scyphozoan clade Rhizostomeae (*Stomolophus meleagris* + *Catostylus mosaicus*, 418–208 mya). Our results suggest the birhopaloid, with its modest increase in cnidocyte shaft complexity, evolved at least three times in the Phanerozoic.

3.3.3 | Stenoteles

Stenoteles are an iconic cnidocyte featuring prominent armature and are capable of envenomation. This cnidocyte type possesses both a long thread as well as a shaft of similar length to the capsule divided by a central constriction. It is distinguished from other cnidocytes by the sizable anchor-like spines known as stylets along the proximal end of the shaft (Tardent, 1995). Östman (2000) considered stenoteles a Hydrozoan novelty, and our results lend strong support ($p = .91$) to this hypothesis. There are isolated reports of stenoteles outside of the Hydrozoa, but these papers either lack images of this cell type (Carrette et al., 2014) or the images they provide lack the necessary stylets (Cengiz & Killi, 2021). There is little support for stenoteles in the last common ancestor of Medusozoa ($p = .13$), suggesting any similarity between "stenoteles" in hydrozoans and nonhydrozoans (assuming they exist at all in the latter) is a case of convergent evolution. Given the current data, we prefer the hypothesis that stenoteles, with their increase in armature complexity, evolved once in the Neoproterozoic.

3.3.4 | Anisorhiza

Very similar in morphology to isorhiza, the anisorhiza is differentiated by a nonisodiametric thread with a slight taper from capsule to tip. This cnidocyte is present sporadically in the Medusozoa, with no support for it being present in the last common ancestor. The earliest appearance of this cell type is in the Siphonophora (*Agalma clausi* + *Physalia physalis*; 469–390 mya). Our results suggest the anisorhiza, with its modest change in thread morphology, evolved anywhere from 5 to 9 times in the Phanerozoic.

3.3.5 | Pseudostenoteles

Pseudostenoteles are differentiated from stenoteles by the lack of a prominent constriction in the shaft, which may taper more gradually toward the thread (Bouillon et al., 1986). Like stenoteles, pseudostenoteles generally possess three sizable spines, however they may display additional rows of spines along the shaft body. Our data suggest that no species possesses both stenoteles and pseudostenoteles, pseudostenoteles being found exclusively within the Leptothecata (*Lafoea dumosa* + *A. filicula*; 471–408 mya), where stenoteles have been lost. The earliest appearance is in the genus *Halecium* (*Halecium mediterraneum* + *Halecium beanii*; 290–199 mya). Our results suggest that the pseudostenotele is a subtype of the stenotele, which evolved once in the Neoproterozoic.

3.3.6 | Rhopalonemes (acrophores and anacrophores)

Rhopalonemes are thought to be siphonophore-specific novelties that function as adhesive "clubs" for catching prey (Bouillon et al., 2004; Damian-Serrano et al., 2021). The shaft is much larger in volume than the capsule, and acrophores and anacrophores can be distinguished by the presence of a small thread at the top of the shaft in the former. Our analysis confirms previous results from Damian-Serrano et al. (2021), with the acrophore subtype present in the Physonectae (*Marrus orthocanna* + *Agalma elegans*; 434–299 mya) and the anacrophore subtype present in the Calycophorae (*Praya dubia* + *Lensia conoidea*; 411–282 mya). Both cnidocytes appear to be highly conserved, with little evidence of loss in our data set. Our results suggest the rhopalonemes, with their major change in cnidocyte shaft and thread morphology, evolved once in the Phanerozoic.

3.3.7 | Desmonemes

Desmonemes possess a prominent thread, which coils into a corkscrew formation at discharge that has been observed to ensnare (Carlgren, 1912; Purcell, 1984) and/or adhere to prey (Damian-Serrano et al., 2021). In our analysis, desmonemes are unique to the Hydrozoan subclass Hydroidolina (*Asyncoryne ryniensis* + *A. filicula*; 566–508 mya) with strong support for the cell type being present in the last common ancestor ($p = 1$). Desmonemes are broadly conserved in Hydroidolina except for a few notable losses including the Leptothecata, the genus *Eudendrium* (*Eudendrium racemosum* + *Eudendrium californicum*; 352–124 mya) and a subset of Capitata (*Cladocoryne floccosa* + *A. ryniensis*; 244–162 mya). Our analysis supports one case of convergent evolution of desmonemes in the thecate hydroid *Amphinema dinema*, but we note the placement of this species in our tree (within the Leptothecata) disagrees with traditional taxonomy. We therefore suggest that desmonenes, with their modified thread morphology, evolved once around the Neoproterozoic/Phanerozoic boundary.

3.4 | A more conservative molecular clock provides corroborates the Ediacaran radiation of cnidocytes

One of the big takeaways from our results is that five, perhaps six cnidocyte types can trace their origin to the Neoproterozoic (isorhizas, mastigophores, spirocysts, euryteles, stenoteles, and possibly desmonemes). Some paleontologists might express reservations with this conclusion, given our estimate for cnidarian origins at ~730–656 mya and the lack of clear cnidarian fossils during this time interval. We therefore performed a second molecular clock analysis using a more conservative model for the rate of molecular evolution, and added hard lower bounds for the age of cnidarians, bilaterians, and animals based on recommendations from the Fossil Calibration Database (Benton et al., 2015). The results of this clock are provided in Figure 3. Despite substantially younger fossil calibrations, the genetic data strongly supports Neoproterozoic origins for the Anthozoa and

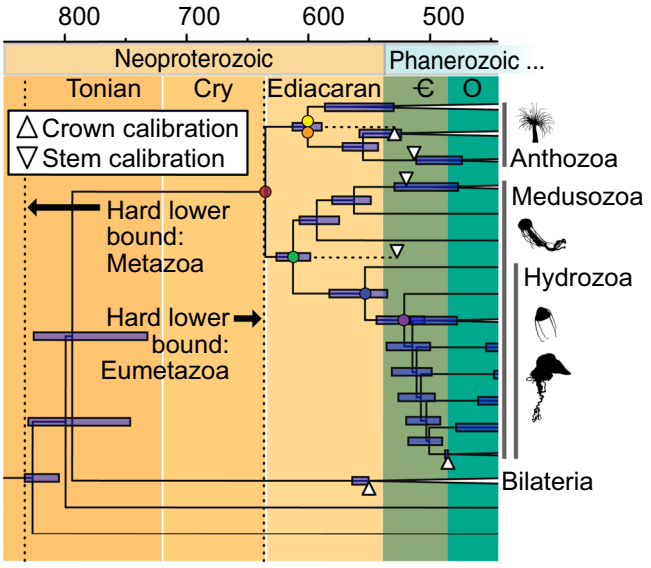

FIGURE 3 The results of a conservative molecular clock analysis, with a focus on the Neoproterozoic through Ordovician. The placement of fossil calibrations is noted with triangles. Cry, Cryogenian; Є, Cambrian; O, Ordovician.

Medusozoa, with the ancestral cnidarian pressing against the hard lower bound. While the timing of animal evolution is notably truncated in this scenario, the timing of early cnidocyte evolution is largely unchanged. We still recover isorhiza, mastigophores, euryteles, spirocysts, and stenoteles evolving in the Ediacaran. Desmonemes may have also evolved in the late Ediacaran, although, like the former analysis, most of the 95% confidence interval rests in the Cambrian. This suggests our major finding—the Neoproterozoic radiation of cnidocyte forms—is robust to variations in the molecular clock analysis.

4 | DISCUSSION

The goal of this paper is to reconstruct the evolution of stinging cells in the Cnidaria, testing the hypothesis that the first cnidocytes were used for the capture of animal prey. Looking at living cnidarians the answer seems obvious; nearly all species contain cnidocytes and nearly all of them use cnidocytes to capture animal prey. However, cnidarians are thought to have evolved before the diversification of most major animal lineages. There is some support for this hypothesis in the fossil record; while most animal phyla make their first, unambiguous appearance in the Cambrian (~541–485 Ma), the medusozoan *Auroralumina attenboroughii* is found in the late Ediacaran (~557–562 mya) with a variety of other putative cnidarian fossils stretching back to ~580 mya (Chen et al., 2000; Dunn et al., 2022; Liu et al., 2014). Additional evidence comes from molecular clock studies, which consistently place crown group cnidarians in the Ediacaran or earlier (Dohrmann & Wörheide, 2017; dos Reis et al., 2015; Erwin et al., 2011; Gold et al., 2015). This temporal discrepancy between the first cnidarians and the diversification of their prey was the impetus of this study.

Using ancestral state reconstruction, our study supports the hypothesis that the earliest cnidarians contained isorhiza—the least specialized and morphologically simplest cnidocyte. When used in prey capture, isorhiza are most abundant in species specializing on soft bodied prey (Carrette et al., 2002; Jarms et al., 2002; Mariscal, 1974b; Purcell, 1984; Purcell & Mills, 1988; although properties between isorhiza subtypes can be dramatic and are perhaps underappreciated, see Colin & Costello, 2007). This is consistent with the fossil record, as mineralized animals do not become common until the Cambrian. It is also quite possible that the first cnidocytes were only minimally involved in prey capture; modern isorhiza serve a diverse set of nonpredatory functions, including intraspecific competition (Kass-Simon & Scappaticci, 2002), defense (Bouillon et al., 1986) locomotion (Ewer & Fox, 1947) and adhesion (Amano et al., 1997). Antibody work on *Hydra* suggests that atrichous isorhizas have adhesive materials similar to the mucous granules of the basal disk, allowing the isorhiza to help anchor the organism while providing an additional mechanism for capturing small prey (Amano et al., 1997). Competition for space may have been a critical selective force for early cnidarians. The earliest known fossil communities of large organisms—which includes putative cnidarians and sea sponges—were benthic, and competition for space appears to have been an important driver of their morphology and distribution (Dunn et al., 2021; Ghisalberti et al., 2014; Sperling et al., 2011). The first cnidarians may have ultimately used their cnidocytes to anchor themselves to the sediment and fight off competitors as much as—or instead of—using them for the capture of soft bodied prey.

Our results also support the rapid appearance of predatory cnidocytes through the Ediacaran, including anthozoan spirocysts and mastigophores, medusozoan euryteles, and hydrozoan stenoteles and desmonemes. The expansion of cnidocyte types is consistent with current differences in ecology and feeding behavior within the major groups. In living anthozoan hexacorals, spirocysts and mastigophores are often found together in specialized feeding tentacles, with the adhesive spirocysts ensnaring the prey (Mariscal, McLean, et al., 1977) and the barbed mastigophores delivering toxins (Kass-Simon & Scappaticci, 2002). This is distinct from sweeper tentacles found in some hexacorals, which are specialized for inter- and intraspecies competition and are composed largely of isorhiza (Kass-Simon & Scappaticci, 2002). Feeding tentacles allow anthozoans to catch large animals and is one of the adaptations that permits the large size of sea anemones compared to other cnidarian polyps. The rise of large anthozoans in the Ediacaran with cnidocytes specialized for larger prey is consistent with a growing body of evidence that larege mobile animals were diversifying at this time, at least on the seafloor (Bobrovskiy et al., 2018; Parry et al., 2017; Runnegar, 2022).

In contrast, the polyps of medusozoans are generally small and only specialize in large prey during the swimming medusa life stage. Euryteles, which likely evolved in the first medusozoans, are specialized for cracking animal exoskeletons (Colin & Costello, 2007; David et al., 2008; Yanagihara et al., 2002). Hydrozoans—the most numerous and diverse clade in the Medusozoa—evolved the desmonemes and stenoteles, which like anthozoan spirocysts and mastigophores combine an adhesive cnidocyte type with a penetrating type

(Kass-Simon & Scappaticci, 2002). In *Hydra*, desmonemes have been shown to work together with stenoteles (Kass-Simon & Scappaticci, 2002; Purcell, 1984) by lassoing prey; the mechanical action of the struggling prey then triggers the discharge of venomous stenoteles (Kass-Simon & Scappaticci, 2002). Tardent (1995) details the penetrating function of stenoteles, which crack a hole in the exoskeletons of prey and are then ejected by the unfurling of the heavy stylets (spines) of the distal shaft. This ejection allows the remainder of the tubule to unfurl into the hole to deliver venom through the open tubule tip. While the fossil record provides little evidence for pelagic animals before the Cambrian (Gold, 2018), molecular work suggests that swimming euarthropod larvae were likely present in the Ediacaran (Wolfe, 2017). This coevolution of exoskeleton-cracking cnidocytes and a pelagic life stage in early Medusozoa supports the hypothesis that a radiation of swimming animals had begun by the Ediacaran.

This study is not focused on the origin of novel cell types like cnidocytes, but our work provides some insight on how the subject could be approached. One outstanding question is whether horizontal gene transfer plays a major role in novel cell type evolution. The striking similarities between cnidocytes and the extrusive organelles found in some other eukaryotes has led some scientists to support a symbiogenic origin (Hwang et al., 2008; Shostak, 1993). In potential support of this idea, early studies of cnidocyte gene expression found a high proportion of genes that were unknown in other animals, with some showing sequence similarity to other eukaryotes and/or bacteria (Hwang et al., 2007). The most compelling example of horizontal gene transfer in cnidocytes comes from the *pgsAA* gene, which is responsible for the poly-γ-glutamate polymer that allows cnidocytes to swell and discharge (Denker et al., 2008). However, the transfer of *pgsAA* from bacteria to animals is not cnidarian-specific, and is therefore not evidence that cnidocytes themselves arose through horizontal transfer. More recent analyses that look wholistically at gene expression show that the cnidocyte's transcriptional regulation is similar to the neuron (Chari et al., 2021; Link et al., 2023; Siebert et al., 2019; Steger et al., 2022) and that a small number of genes can change the cell fate from neuron to cnidocyte (Babonis et al., 2022). This is consistent with an alternative hypothesis that cnidocytes and neurons share a common ancestor (Galliot & Quiquand, 2011). But these analyses generally focus on what is shared between cell types, not what is different. So while wholesale endosymbiosis is not supported by current evidence, it is still possible that horizontal gene transfer played an important role in the evolution of cnidocytes, and organisms with cnidocyte-like extrusive organelles could have been an important source of these genes. But for that to be the case, these extrusive organelles would have to predate the origin of cnidocytes in the late-Neoproterozoic. Dinoflagellates, for example, did not evolve until the mid-Phanerozoic (Riding et al., 2022), meaning the cnidocyte-like organelles of some species (Hwang et al., 2008) cannot be ancestral to cnidarian stinging cells. When other extrusive organelles described in ciliates and flagellates evolved is less clear. One could use a technique similar to this study to trace the evolution of these organelles and determine if any date back to the Neoproterozoic or earlier. If so, focusing on the genetics of these eukaryotes could reveal the origin of important components of cnidocyte development.

As a final point on cell type evolution, our results suggest the mastigophore could be a good candidate for studying how complex cell types convergently evolve. Most of the cnidocytes in our data set evolved only once, and those that did evolve multiple times are generally defined by their lack of a trait found in other cnidocytes (e.g., anisorhiza and amastigophores). The exception to this appears to be the mastigophore and the birhopaloid. Birhopaloids, with their dual swellings along the capsule shaft, represent a modest increase in complexity, but they are rare in cnidarians (Supporting Information S1: Figure S5). Mastigophores, on the other hand, are widespread (Supporting Information S1: Figure S9) and present in a variety of model cnidarians including *Nematostella*, *Clytia*, *Carybdea*, and *Craspedacusta*. According to our ancestral state reconstruction, the mastigophores from all these organisms evolved independently. Assuming the isorhiza represents the ancestral cnidocyte type, the well-defined and often heavily armored shaft of the mastigophore represents a clear increase in cell complexity associated with prey capture. Elucidating how the mastigophore—and cnidocytes more broadly—evolved into so many nuanced and diverse types will inform us how complex cell types originate and diversify over deep time.

5 | CONCLUSIONS

By reconstructing the evolutionary history of cnidarian stinging cells, we present a hypothesis regarding the Precambrian rise of animal predation. The earliest, Cryogenian-age cnidarians were likely small, benthic animals (Kayal et al., 2018) that used a simple cnidocyte type (the isorhiza) to compete for space on the ocean floor and perhaps capture small, soft bodied prey. As animals diversified and increased in size during the Ediacaran, cnidarians took two distinct approaches to

taking advantage of this food source. Anthozoans became larger and developed the spirocysts and mastigophores, which are combined in the feeding tentacles of many sea anemones. Medusozoans developed a swimming life stage with a different set of specialized cnidocytes—the euryteles, desmonemes, and stenoteles—which allow for the ensnaring of prey and cracking of exoskeletons. This allowed for specialization on swimming arthropods and other pelagic prey. Our results support the hypothesis that animal diversification has a Precambrian origin, and suggest the cnidaria had a significant impact on the early evolution and trajectory of food webs and ecological structure.

ACKNOWLEDGMENTS

We thank Todd Oakley and Natasha Picciani for their help using and updating their data. We also thank Todd Oakley, Celina Juliano, Rachael Bay, and Chris Mulligan for valuable feedback on earlier versions of the manuscript. This work was supported by a National Science Foundation Graduate Research Fellowship (Noémie C. Sierra) and National Science Foundation grant 2044871 (David A. Gold).

CONFLICT OF INTEREST STATEMENT

The authors declare no conflict of interest.

DATA AVAILABILITY STATEMENT

The data that support the findings of this study are openly available in GitHub at https://github.com/DavidGoldLab/2023_Cnidocyte_Ancestral_State, reference number https://doi.org/10.5281/zenodo.10198840.

ORCID

Noémie C. Sierra http://orcid.org/0000-0003-1329-4733
David A. Gold http://orcid.org/0000-0003-0135-4022

REFERENCES

Amano, H., Koizumi, O., & Kobayakawa, Y. (1997). Morphogenesis of the atrichous isorhiza, a type of nematocyst, in Hydra observed with a monoclonal antibody. *Development Genes and Evolution*, *207*, 413–416.

Americus, B., Lotan, T., Bartholomew, J. L., & Atkinson, S. D. (2020). A comparison of the structure and function of nematocysts in free-living and parasitic cnidarians (Myxozoa). *International Journal for Parasitology*, *50*, 763–769.

Babonis, L. S., Enjolras, C., Ryan, J. F., & Martindale, M. Q. (2022). A novel regulatory gene promotes novel cell fate by suppressing ancestral fate in the sea anemone *Nematostella vectensis*. *Proceedings of the National Academy of Sciences United States of America*, *119*, e2113701119.

Babonis, L. S., & Martindale, M. Q. (2014). Old cell, new trick? Cnidocytes as a model for the evolution of novelty. *Integrative and Comparative Biology*, *54*(4), 714–722.

Baron-Szabo, R. C., Schafhauser, A., Götz, S., & Stinnesbeck, W. (2006). Scleractinian corals from the cardenas formation (Maastrichtian), San Luis potosí, Mexico. *Journal of Paleontology*, *80*, 1033–1046.

Beaulieu, J., O'Meara, B., Oliver, J., & Boyko, J. (2020). *CorHMM: Hidden Markov models of character evolution*. R Package Version.

Ben-David, J., Atkinson, S. D., Pollak, Y., Yossifon, G., Shavit, U., Bartholomew, J. L., & Lotan, T. (2016). Myxozoan polar tubules display structural and functional variation. *Parasites & Vectors*, *9*, 549.

Benton, M., Donoghue, P., Vinther, J., Asher, R., Friedman, M., & Near, T. (2015). Constraints on the timescale of animal evolutionary history. *Palaeontologia Electronica*, *18*, 1–106.

Bobrovskiy, I., Hope, J. M., Ivantsov, A., Nettersheim, B. J., Hallmann, C., & Brocks, J. J. (2018). Ancient steroids establish the Ediacaran fossil Dickinsonia as one of the earliest animals. *Science*, *361*, 1246–1249.

Bouillon, J., Boero, F., & Gravier-Bonnet, N. (1986). Pseudostenotele, a new type of nematocyst, and its phylogenetic meaning within the Haleciidae (Cnidaria, Hydrozoa). *Indo-Malayan Zoology*, *3*, 63–69.

Bouillon, J., Medel, M. D., Pagès, F., Gili, J.-M., Boero, F., & Gravili, C. (2004). Fauna of the Mediterranean hydrozoa. *Scientia Marina*, *68*, 5–438.

Boyko, J. D., & Beaulieu, J. M. (2021). Generalized hidden Markov models for phylogenetic comparative datasets. *Methods in Ecology and Evolution*, *12*, 468–478.

Carlgren, O. H. (1912). *Ceriantharia (B. Luno)*. Danish Ingolf-Expedition.

Carlgren, O. H. (1940). *A contribution to the knowledge of the structure and distribution of the Cnidae in the Anthozoa. (CWK Gleerup)*. Kungliga Fysiografiska sällskapets i Lund handlingar N. F.

Carrette, T., Alderslade, P., & Seymour, J. (2002). Nematocyst ratio and prey in two Australian cubomedusans, *Chironex fleckeri* and Chiropsalmus sp. *Toxicon*, *40*, 1547–1551.

Carrette, T., Straehler-Pohl, I., & Seymour, J. (2014). Early life history of Alatina cf. moseri populations from Australia and Hawaii with implications for taxonomy (Cubozoa: Carybdeida, Alatinidae). *PLoS One*, *9*, e84377.

Cengiz, S., & Killi, N. (2021). Nematocysts types and morphological features of some scyphozoa species in the Southwest Turkey. *Fresenius Environmental Bulletin*, *30*, 32–40.

Chari, T., Weissbourd, B., Gehring, J., Ferraioli, A., Leclère, L., Herl, M., Gao, F., Chevalier, S., Copley, R. R., Houliston, E., Anderson, D. J., & Pachter, L. (2021). Whole-animal multiplexed single-cell RNA-seq reveals transcriptional shifts across Clytia medusa cell types. *Science Advances*, *7*, eabh1683.

Chen, J.-Y., Oliveri, P., Li, C.-W., Zhou, G.-Q., Gao, F., Hagadorn, J. W., Peterson, K. J., & Davidson, E. H. (2000). Precambrian animal diversity: putative phosphatized embryos from the Doushantuo Formation of China. *Proceedings of the National Academy of Sciences United States of America*, *97*, 4457–4462.

Colin, S. P., & Costello, J. H. (2007). Functional characteristics of nematocysts found on the scyphomedusa *Cyanea capillata*. *Journal of Experimental Marine Biology and Ecology*, *351*, 114–120.

Columbus-Shenkar, Y. Y., Sachkova, M. Y., Macrander, J., Fridrich, A., Modepalli, V., Reitzel, A. M., Sunagar, K., & Moran, Y. (2018). Dynamics of venom composition across a complex life cycle. *eLife*, *7*, e35014.

Cutress, C. E. (1955). An interpretation of the structure and distribution of cnidae in Anthozoa. *Systematic Zoology*, *4*, 120–137.

Damian-Serrano, A., Haddock, S. H., & Dunn, C. W. (2021). The evolution of siphonophore tentilla for specialized prey capture in the open ocean. *Proceedings of the National Academy of Sciences United States of America*, *118*, e2005063118.

David, C. N., Özbek, S., Adamczyk, P., Meier, S., Pauly, B., Chapman, J., Hwang, J. S., Gojobori, T., & Holstein, T. W. (2008). Evolution of complex structures: Minicollagens shape the cnidarian nematocyst. *Trends in Genetics*, *24*, 431–438.

Denker, E., Bapteste, E., Le Guyader, H., Manuel, M., & Rabet, N. (2008). Horizontal gene transfer and the evolution of cnidarian stinging cells. *Current Biology*, *18*, R858–R859.

Dohrmann, M., & Wörheide, G. (2017). Dating early animal evolution using phylogenomic data. *Scientific Reports*, *7*, 3599.

Dong, X.-P., Cunningham, J. A., Bengtson, S., Thomas, C.-W., Liu, J., Stampanoni, M., & Donoghue, P. C. (2013). Embryos, polyps and medusae of the Early Cambrian scyphozoan Olivooides. *Proceedings of the Royal Society B: Biological Sciences*, *280*, 20130071.

dos Reis, M., Thawornwattana, Y., Angelis, K., Telford, M. J., Donoghue, P. C. J., & Yang, Z. (2015). Uncertainty in the timing of origin of animals and the limits of precision in molecular timescales. *Current Biology*, *25*, 2939–2950.

Dunn, F. S., Kenchington, C. G., Parry, L. A., Clark, J. W., Kendall, R. S., & Wilby, P. R. (2022). A crown-group cnidarian from the Ediacaran of Charnwood Forest. *Nature Ecology & Evolution*, *6*, 1095–1104.

Dunn, F. S., Liu, A. G., Grazhdankin, D. V., Vixseboxse, P., Flannery-Sutherland, J., Green, E., Harris, S., Wilby, P. R., & Donoghue, P. C. J. (2021). The developmental biology of Charnia and the eumetazoan affinity of the Ediacaran rangeomorphs. *Science Advances*, *7*, eabe0291.

Erwin, D. H., Laflamme, M., Tweedt, S. M., Sperling, E. A., Pisani, D., & Peterson, K. J. (2011). The Cambrian conundrum: Early divergence and later ecological success in the early history of animals. *Science*, *334*, 1091–1097.

Ewer, R. F., & Fox, H. M. (1947). On the functions and mode of action of the nematocysts of Hydra. *Proceedings of the Zoological Society of London*, *117*, 365–376.

Ezaki, Y. (2000). Palaeoecological and phylogenetic implications of a new scleractiniamorph genus from Permian sponge reefs, South China. *Palaeontology*, *43*, 199–217.

Fautin, D. G. (2009). Structural diversity, systematics, and evolution of cnidae. *Toxicon*, *54*, 1054–1064.

Fedonkin, M. A., & Waggoner, B. M. (1997). The Late Precambrian fossil Kimberella is a mollusc-like bilaterian organism. *Nature*, *388*, 868–871.

Fuller, M., & Jenkins, R. (2007). Reef corals from the lower Cambrian of the Flinders Ranges, South Australia. *Palaeontology*, *50*, 961–980.

Galliot, B., & Quiquand, M. (2011). A two-step process in the emergence of neurogenesis. *European Journal of Neuroscience*, *34*, 847–862.

Garm, A., Lebouvier, M., & Tolunay, D. (2015). Mating in the box jellyfish C opula sivickisi—Novel function of cnidocytes. *Journal of Morphology*, *276*, 1055–1064.

Gershwin, L.-A. (2006). Nematocysts of the cubozoa. *Zootaxa*, *1232*, 1.

Ghisalberti, M., Gold, D. A., Laflamme, M., Clapham, M. E., Narbonne, G. M., Summons, R. E., Johnston, D. T., & Jacobs, D. K. (2014). Canopy flow analysis reveals the advantage of size in the oldest communities of multicellular eukaryotes. *Current Biology*, *24*, 305–309.

Gold, D. A. (2018). Life in changing fluids: A critical appraisal of swimming animals before the Cambrian. *Integrative and Comparative Biology*, *58*, 677–687.

Gold, D. A., Katsuki, T., Li, Y., Yan, X., Regulski, M., Ibberson, D., Holstein, T., Steele, R. E., Jacobs, D. K., & Greenspan, R. J. (2019). The genome of the jellyfish Aurelia and the evolution of animal complexity. *Nature Ecology & Evolution*, *3*, 96–104.

Gold, D. A., Runnegar, B., Gehling, J. G., & Jacobs, D. K. (2015). Ancestral state reconstruction of ontogeny supports a bilaterian affinity for Dickinsonia. *Evolution & Development*, *17*, 315–324.

Han, J., Hu, S., Cartwright, P., Zhao, F., Ou, Q., Kubota, S., Wang, X., & Yang, X. (2016). The earliest pelagic jellyfish with rhopalia from Cambrian Chengjiang Lagerstätte. *Palaeogeography, Palaeoclimatology, Palaeoecology*, *449*, 166–173.

Han, J., Kubota, S., Uchida, H., Stanley Jr., G. D., Yao, X., Shu, D., Li, Y., & Yasui, K. (2010). Tiny sea anemone from the lower Cambrian of China. *PLoS One*, *5*, e13276.

Hwang, J. S., Nagai, S., Hayakawa, S., Takaku, Y., & Gojobori, T. (2008). The search for the origin of cnidarian nematocysts in dinoflagellates. In P. Pontarotti (Ed.), *Evolutionary biology from concept to application* (pp. 135–152). Springer Berlin Heidelberg.

Hwang, J. S., Ohyanagi, H., Hayakawa, S., Osato, N., Nishimiya-Fujisawa, C., Ikeo, K., David, C. N., Fujisawa, T., & Gojobori, T. (2007). The evolutionary emergence of cell type-specific genes inferred from the gene expression analysis of Hydra. *Proceedings of the National Academy of Sciences United States of America*, *104*, 14735–14740.

Iten, H. V., Leme, J. M., Pacheco, M. L., Simões, M. G., Fairchild, T. R., Rodrigues, F., Galante, D., Boggiani, P. C., & Marques, A. C. (2016). Origin and early diversification of phylum Cnidaria: Key macrofossils from the Ediacaran System of North and South America. In S. Goffredo & Z. Dubinsky (Eds.), *The Cnidaria, past, present and future: The world of medusa and her sisters* (pp. 31–40). Springer.

Jarms, G., Tiemann, H., & Båmstedt, U. (2002). Development and biology of *Periphylla periphylla* (Scyphozoa: Coronatae) in a Norwegian fjord. *Marine Biology*, *141*, 647–657.

Jell, J. S., Cook, A. G., & Jell, P. A. (2011). Australian cretaceous cnidaria and porifera. *Alcheringa: An Australasian Journal of Palaeontology*, *35*, 241–284.

Johnson, R. G., & Richardson, E. S. (1968). *Pennsylvanian invertebrates of the Mazon Creek area*. The Essex Fauna and Medusae.

Kalyaanamoorthy, S., Minh, B. Q., Wong, T. K. F., Von Haeseler, A., & Jermiin, L. S. (2017). ModelFinder: Fast model selection for accurate phylogenetic estimates. *Nature Methods*, *14*, 587–589.

Kass-Simon, G., & Scappaticci, Jr, A. A. (2002). The behavioral and developmental physiology of nematocysts. *Canadian Journal of Zoology*, *80*, 1772–1794.

Kayal, E., Bentlage, B., Sabrina Pankey, M., Ohdera, A. H., Medina, M., Plachetzki, D. C., Collins, A. G., & Ryan, J. F. (2018). Phylogenomics provides a robust topology of the major cnidarian lineages and insights on the origins of key organismal traits. *BMC Evolutionary Biology*, *18*, 68.

Laumer, C. E., Fernández, R., Lemer, S., Combosch, D., Kocot, K. M., Riesgo, A., Andrade, S. C., Sterrer, W., Sørensen, M. V., & Giribet, G. (2019). Revisiting metazoan phylogeny with genomic sampling of all phyla. *Proceedings of the Royal Society B*, *286*, 20190831.

Leclère, L., Horin, C., Chevalier, S., Lapébie, P., Dru, P., Peron, S., Jager, M., Condamine, T., Pottin, K., Romano, S., Steger, J., Sinigaglia, C., Barreau, C., Quiroga Artigas, G., Ruggiero, A., Fourrage, C., Kraus, J., Poulain, J., Aury, J. M., ... Copley, R. R. (2019). The genome of the jellyfish *Clytia hemisphaerica* and the evolution of the cnidarian life-cycle. *Nature Ecology & Evolution*, *3*, 801–810.

Link, O., Jahnel, S. M., Janicek, K., Kraus, J., Montenegro, J. D., Zimmerman, B., Cole, A. G., & Technau, U. (2023). A cell-type atlas from a scyphozoan jellyfish *Aurelia coerulea* (formerly sp. 1) provides insights into changes of cell-type diversity in the transition from polyps to medusae. *bioRxiv*. https://doi.org/10.1101/2023.08.24.554571

Liu, A. G., Matthews, J. J., Menon, L. R., McIlroy, D., & Brasier, M. D. (2014). Haootia quadriformis n. gen., n. sp., interpreted as a muscular cnidarian impression from the Late Ediacaran period (approx. 560 Ma). *Proceeding of Biological Science*, *281*, 20141202.

Mariscal, R. N. (1974a). Scanning electron microscopy of the sensory surface of the tentacles of sea anemones and corals. *Zeitschrift für Zellforschung und Mikroskopische Anatomie*, *147*, 149–156.

Mariscal, R. N. (1974b). "Nematocysts," in coelenterate. In L. Muscatine & H. M. Lenhoff (Eds.), *Biology* (pp. 129–178). Academic Press.

Mariscal, R. N., Conklin, E. J., & Bigger, C. H. (1977). The ptychocyst, a major new category of cnida used in tube construction by a cerianthid anemone. *The Biological Bulletin*, *152*, 392–405.

Mariscal, R. N., McLean, R. B., & Hand, C. (1977). The form and function of cnidarian spirocysts. *Cell and Tissue Research*, *178*, 427–433.

Minh, B. Q., Schmidt, H. A., Chernomor, O., Schrempf, D., Woodhams, M. D., Von Haeseler, A., & Lanfear, R. (2020). IQ-TREE 2: New models and efficient methods for phylogenetic inference in the genomic era. *Molecular Biology and Evolution*, *37*, 1530–1534.

Nüchter, T., Benoit, M., Engel, U., Özbek, S., & Holstein, T. W. (2006). Nanosecond-scale kinetics of nematocyst discharge. *Current Biology*, *16*, R316–R318.

Östman, C. (2000). A guideline to nematocyst nomenclature and classification, and some notes on the systematic value of nematocysts. *Scientia Marina*, *64*, 31–46.

Parry, L. A., Boggiani, P. C., Condon, D. J., Garwood, R. J., Leme, J. M., Mcilroy, D., Brasier, M. D., Trindade, R., Campanha, G., Pacheco, M., Diniz, C., & Liu, A. G. (2017). Ichnological evidence for meiofaunal bilaterians from the terminal Ediacaran and earliest Cambrian of Brazil. *Nature Ecology & Evolution*, *1*, 1455–1464.

Picciani, N., Kerlin, J. R., Sierra, N., Swafford, A. J. M., Ramirez, M. D., Roberts, N. G., Cannon, J. T., Daly, M., & Oakley, T. H. (2018). Prolific origination of eyes in Cnidaria with co-option of non-visual opsins. *Current Biology*, *28*, 2413–2419.

Purcell, J. E. (1984). The functions of nematocysts in prey capture by epipelagic siphonophores (Coelenterata, Hydrozoa). *The Biological Bulletin*, *166*, 310–327.

Purcell, J. E., & Mills, C. E. (1988). The correlation of nematocyst types to diets in pelagic Hydrozoa. In D. A. Hessinger & H. M. Lenhoff (Eds.), *The biology of nematocysts* (pp. 463–485). Academic Press.

Revell, L. J. (2014). *Package "phytools": Phylogenetic tools for comparative biology (and other things)*. http://cran.r-project.org/package=phytools

Riding, J. B., Fensome, R. A., Soyer-Gobillard, M. O., & Medlin, L. K. (2022). A review of the dinoflagellates and their evolution from fossils to modern. *Journal of Marine Science and Engineering*, *11*, 1.

Rifkin, J. F. (1991). A study of the spirocytes from the Ceriantharia and Actiniaria (Cnidaria: Anthozoa). *Cell and Tissue Research*, *266*, 365–373.

Runnegar, B. (2022). Following the logic behind biological interpretations of the Ediacaran biotas. *Geological Magazine*, *159*, 1093–1117.

Schmidt, H. (1974). On evolution in the Anthozoa, *Proceedings of the Second International Coral Reef Symposium, 1974* (pp. 533–560). Great Barrier Reef Committee.

Shostak, S. (1993). A symbiogenetic theory for the origins of cnidocysts in Cnidaria. *Biosystems*, *29*(1), 49–58.

Siddall, M. E., Martin, D. S., Bridge, D., Desser, S. S., & Cone, D. K. (1995). The demise of a phylum of protists: Phylogeny of Myxozoa and other parasitic Cnidaria. *The Journal of Parasitology*, *81*, 961–967.

Siebert, S., Farrell, J. A., Cazet, J. F., Abeykoon, Y., Primack, A. S., Schnitzler, C. E., & Juliano, C. E. (2019). Stem cell differentiation trajectories in Hydra resolved at single-cell resolution. *Science*, *365*, eaav9314.

Song, X., Ruthensteiner, B., Lyu, M., Liu, X., Wang, J., & Han, J. (2021). Advanced Cambrian hydroid fossils (Cnidaria: Hydrozoa) extend the medusozoan evolutionary history. *Proceedings of the Royal Society B*, *288*, 20202939.

Sperling, E. A., Peterson, K. J., & Laflamme, M. (2011). Rangeomorphs, Thectardis (Porifera?) and dissolved organic carbon in the Ediacaran oceans: Rangeomorphs, Thectardis and DOC. *Geobiology*, *9*, 24–33.

Steger, J., Cole, A. G., Denner, A., Lebedeva, T., Genikhovich, G., Ries, A., Reischl, R., Taudes, E., Lassnig, M., & Technau, U. (2022). Single-cell transcriptomics identifies conserved regulators of neuroglandular lineages. *Cell Reports*, *40*, 111370.

Suchard, M. A., Lemey, P., Baele, G., Ayres, D. L., Drummond, A. J., & Rambaut, A. (2018). Bayesian phylogenetic and phylodynamic data integration using BEAST 1.10. *Virus Evolution*, *4*, vey016.

Tardent, P. (1995). The cnidarian cnidocyte, a hightech cellular weaponry. *BioEssays*, *17*, 351–362.

Wolfe, J. M. (2017). Metamorphosis is ancestral for crown euarthropods, and evolved in the Cambrian or earlier. *Integrative and Comparative Biology*, *57*, 499–509.

Yanagihara, A. A., Kuroiwa, J. M. Y., Oliver, L. M., Chung, J. J., & Kunkel, D. D. (2002). Ultrastructure of a novel eurytele nematocyst of *Carybdea alata* reynaud (Cubozoa, Cnidaria). *Cell and Tissue Research*, *308*, 307–318.

Zapata, F., Goetz, F. E., Smith, S. A., Howison, M., Siebert, S., Church, S. H., Sanders, S. M., Ames, C. L., McFadden, C. S., France, S. C., Daly, M., Collins, A. G., Haddock, S. H. D., Dunn, C. W., & Cartwright, P. (2015). Phylogenomic analyses support traditional relationships within Cnidaria. *PLoS One*, *10*, e0139068.

Zenkert, C., Takahashi, T., Diesner, M. O., & Özbek, S. (2011). Morphological and molecular analysis of the *Nematostella vectensis* cnidom. *PLoS One*, *6*, e22725.

SUPPORTING INFORMATION

Additional supporting information can be found online in the Supporting Information section at the end of this article.

How to cite this article: Sierra, N. C., & Gold, D. A. (2024). The evolution of cnidarian stinging cells supports a Precambrian radiation of animal predators. *Evolution & Development*, *26*, e12469. https://doi.org/10.1111/ede.12469